Available online at BCREC Website: https://bcrec.undip.ac.id

Bulletin of Chemical Reaction Engineering & Catalysis, 13 (3) 2018, 512-519

Research Article

Preparation of 2-Methylnaphthalene from 1-Methylnaphthalene via Catalytic Isomerization and Crystallization

Hao Sun[1*], Kang Sun[1], Jianchun Jiang[1], Zhenggui Gu[2]

[1]*Jiangsu Key Laboratory for Biomass Energy and Material, National Engineering Laboratory for Biomass Chemical Utilization, Institute of Chemical Industry of Forest Products, Chinese Academy of Forestry, Nanjing 210042, China*

[2]*Jiangsu Provincial Key Laboratory of Materials Cycling and Pollution Control, College of Chemistry and Materials Science, Nanjing Normal University, Nanjing 210023, China*

Received: 10th May 2018; Revised: 16th July 2018; Accepted: 17th July 2018; Available online: 14th November 2018; Published regularly: December 2018

Abstract

Large amounts of residual 1-methylnaphthalene are generated when 2-methylnaphthalene is extracted from alkyl naphthalene. In order to transform waste into assets, this study proposes a feasible process for preparing 2-methylnaphthalene from 1-methylnaphthalene through isomerization and crystallization. The 1-methylnaphthalene isomerization was carried out in a fixed-bed reactor over mixed acids-treated HBEA zeolite. The results showed that acidic properties of catalysts and reaction temperature were associated with the 2-methylnaphthalene selectivity, yield and catalytic stability. At a high reaction temperature of 623 K, the 2-methylnaphthalene yield was 65.84 %, and the deactivation rate was much lower. The separation of reaction products was then investigated by two consecutive crystallization processes. Under optimal conditions, the 2-methylnaphthalene purity attained 96.67 % in the product, while the yield was 87.48 % in the refining process.

Keywords:
Modified zeolite; 1-Methylnaphthalene, Isomerization; Crystallization; 2-Methylnaphthalene

How to Cite: Sun, H., Sun, K., Jiang, J., Gu, Z. (2018). Preparation of 2-Methylnaphthalene from 1-Methylnaphthalene via Catalytic Isomerization and Crystallization. *Bulletin of Chemical Reaction Engineering & Catalysis*, 13 (3): 512-519 (doi:10.9767/bcrec.13.3.2650.512-519)

Permalink/DOI: https://doi.org/10.9767/bcrec.13.3.2650.512-519

1. Introduction

The production of C_{10} aromatics are the residual oils after trimethylbenzene and indane are extracted from C_9 aromatics, and have reached more than 300,000 tons per year in China. Using C_{10} aromatics as solvents or fuel oil is both inefficient and polluting, because they are made up of about 30 % alkyl naphthalenes. Among alkyl naphthalenes, 2-methylnaphthalene (2-MN) is a well-known useful intermediate for producing polyethylene naphthalene (PEN) and vitamin K [1-3]. In our previous study [4], 2-MN was attained from alkyl naphthalenes via side-stream distillation and continuous crystallization processes. However, the residual component was mainly 1-methyl-

* Corresponding Author.
E-mail: 15850534739@163.com (H. Sun)
Telp: +86-25-85482484, Fax: +86-25-85482484

naphthalene (1-MN), the industrial demand for which is much lower than that for 2-MN. If we could obtain 2-MN from 1-MN, residual C_{10} aromatics could be maximally utilized with less waste.

Past studies [5-11] have demonstrated HBEA zeolite to be an effective catalyst for 1-MN isomerization owing to its thermal stability, appropriate pore size distribution and high activity in comparison with those of other zeolites. However, due to its initial defective structure, detrimental by-products are unavoidable during the synthesis process, and its catalytic life of isomerization is short. Modifications of zeolites, such as: silylation [12], stream [13], and dealumination [14-17], are advantageous for improving the stability and selectivity of catalytic reaction. Our previous report has studied the HBEA zeolite modified by organic acid [11], and the modified catalyst demonstrated high selectivity for the conversion of alkyl naphthalene. Dealumination is accomplished by hydrolysis of Al–O–Si bonds with inorganic and/or organic acids. It is obvious that the acids used in the treatment are responsible for the acidic properties and catalytic performance of HBEA zeolite. Nevertheless, the mixture of inorganic and organic acids utilized for the dealumination of HBEA and the catalytic deactivation rate of mixed acids-treated zeolite for 1-MN isomerization have scarcely been investigated.

The product of 1-MN isomerization contains both 1-MN and 2-MN due to the thermodynamic equilibrium of isomerization reaction. The components of this mixture have a large difference in melting point, but a small difference in volatility. As reported in our previous study [4], crystallization is an effective method for separating the isomers mixture.

In order to make full use of the 1-MN resulting from residual C_{10} aromatics, this work carried out the 1-MN isomerization over modified HBEA zeolite. The modified zeolite was characterized by various methods, and its catalytic properties were investigated in a fixed-bed reactor. Furthermore, in order to obtain 2-MN with high purity and yield, two-fold crystallization for the separation of methylnaphthalene isomers was also studied.

2. Materials and Methods

2.1 Source of Chemicals

The 1-MN (> 98 % purity) was purchased from Aladdin Industrial Inc., Shanghai, China. Hydrochloric acid and oxalic acid were both analytical regents obtained from Sinopharm Chemical Regent Co., Ltd., Shanghai, China. Parent HBEA zeolite was synthesized by the method described in Matsukata *et al.* [18].

2.2 Catalyst Preparation

The parent HBEA zeolite was activated at 823 K (2 K/min heating rate) for 5 h before the modification. The dealuminated catalyst was prepared by impregnating HBEA zeolite into 0.1 mol/L solution of mixed hydrochloric and oxalic acids (hydrochloric/oxalic = 1) at 343 K for 1 h. After that, the sample was filtered, washed, dried and calcined at 823 K (2 K/min heating rate) for 4 h. The synthesized catalyst was denoted as Mix-HBEA.

2.3 Characterization

X-ray diffraction (XRD) was recorded on a D/max-2500 (Rigaku, Japan) using Cu-Kα radiation and operating at 100 mA and 40 kV. Fourier transform infrared (FTIR) spectroscopy was conducted on a Tensor 27 (Bruker, Germany) spectrometer in the mid-IR region (400-4000 cm^{-1}). Surface acidity was performed with FTIR spectrometry after adsorption of pyridine (Py-FTIR), using a Vertex 70 (Bruker, Germany) spectrometer coupled with a conventional high vacuum system. The molar extinction coefficients for pyridine on the Brönsted (1545 cm^{-1} band, ε_B) and Lewis acid sites (1454 cm^{-1} band, ε_L) were identified as 1.23 cm/μmol and 1.73 cm/μmol, respectively [19]. NH_3 temperature-programmed desorption (NH_3-TPD) was carried out on a TP-5080 (Xianquan, China) instrument equipped with a thermal conductivity detector. Thermogravimetric (TG) analysis was measured using a Diamond TG/DTA (Perkin Elmer, USA) instrument in the presence of oxygen.

2.4 Reaction and Separation

The isomerization of 1-MN was performed in a fixed-bed reactor. After 1.6 g of catalyst was loaded in the center of the reactor, the isomerization was carried out in the presence of nitrogen under atmospheric pressure. The flow-rate of 1-MN and N_2 were 1.3 h^{-1} weight hourly space velocity (WHSV) and 20 mL/min, respectively. Products were sampled and analyzed at regular intervals. The 1-MN conversion was based on the 1-MN concentration change, and 2-MN selectivity was defined as the mass ratio of 2-MN to 1-MN conversion.

A home-made apparatus [20] was then utilized to crystallize and filter the products of the isomerization reaction. This apparatus consists

of a jacketed crystallizer, a homothermal filter and a filtrate collector. The temperature of the apparatus was controlled by a circulating pump, using cold glycol as a cooling medium. The 2-MN yield in the crystallization process was calculated as follows:

$$2-MN\ yield(\%)=\frac{Y_{crystal}.C_{2-MN}}{Y_{2-MN}} \quad (1)$$

where $Y_{2\text{-MN}}$ is the 2-MN yield in the reaction process, Y_{crystal} is the crystal yield of the crystallization process, and $C_{2\text{-MN}}$ is the 2-MN purity of the crystal in the crystallization process.

All samples were quantitatively analyzed by gas chromatography on a Trace 1300 (ThermoFisher, America) using a SE-30 capillary column. A GC-MS (Varian 3800/2200) equipped with a Varian CP-Sil-19 column identified the main components as naphthalene (NA), 1-MN, 2-MN, dimethylnaphthalene (DMN) and polynuclear aromatic.

3. Results and Discussion

3.1 Characterization of Catalyst

The crystal structure and lattice vibration of Mix-HBEA were measured by XRD and FTIR, respectively. The XRD results plotted in Figure 1a show typical reflections of the zeolite HBEA at 7.8° and 22.5°, with no other significant peaks. As shown in Figure 1b, the bands at 1090 and 795 cm^{-1} are associated with the symmetric and asymmetric stretching vibrations of the TO_4 units of zeolite, respectively. At 569 cm^{-1}, the adsorption band represents a characteristic of the BEA framework structure in the Mix-HBEA catalyst [21]. These results suggest that treatment with mixed acids preserves the zeolite structure of HBEA.

NH_3-TPD analysis was carried out to estimated the types and number of acid sites on the surface. The results are depicted in Figure 2a. NH_3 desorption peaks occurred in the ranges of 100-300 °C and 300-700 °C are as-

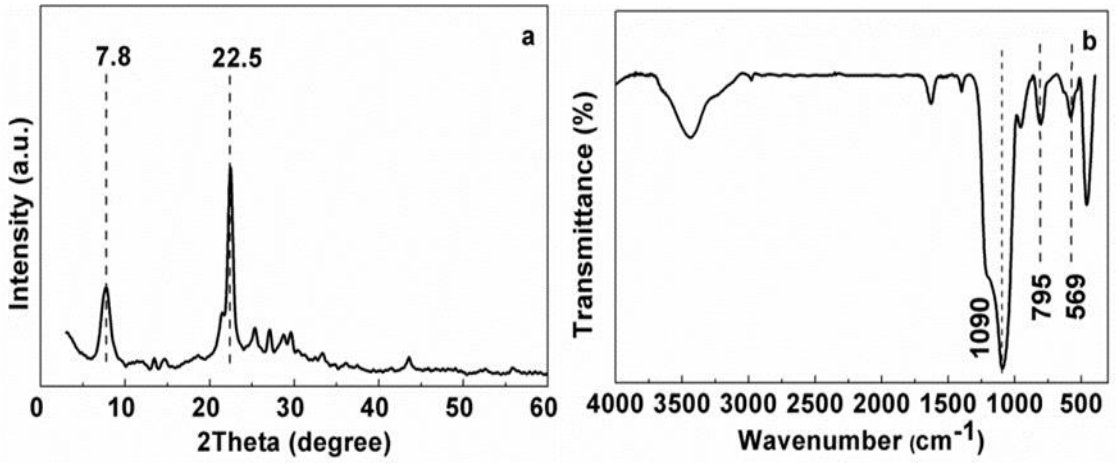

Figure 1. (a) XRD and (b) FTIR patterns of Mix-HBEA catalyst

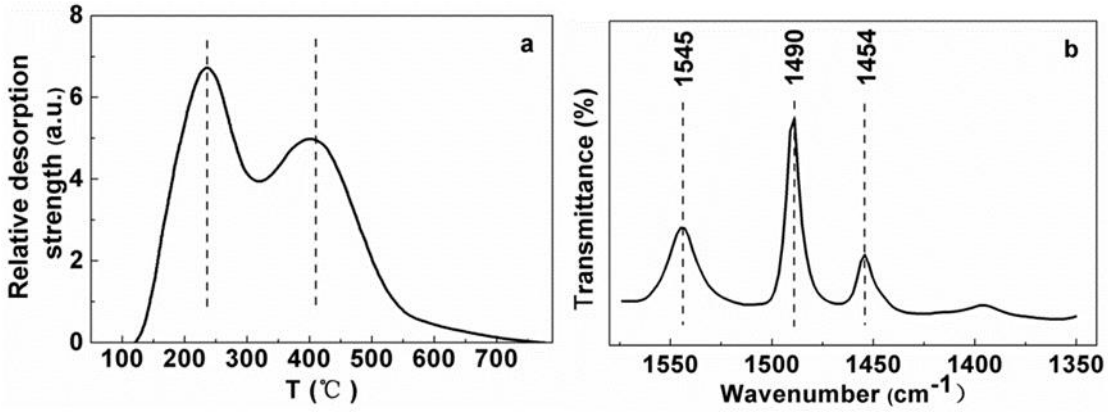

Figure 2. (a) NH_3-TPD curve of Mix-HBEA; (b) FTIR spectra of Mix-HBEA catalyst after desorption of pyridine at 573 K

cribed to weakly acidic sites and strongly acidic sites, respectively [22,23]. The amounts of weak and strong acid were calculated based on the areas of the two peaks, and the results are listed in Table 1. The amount of strong acid is clearly higher than that of weak acid, and these weak acid sites are unable to activate the isomerization reaction [24].

Further information on the strong Brönsted and Lewis acidic properties of Mix-HBEA were then determined through Py-FTIR, and the results are illustrated in Figure 2b. The bands at 1454 and 1545 cm^{-1} are related to pyridine adsorbed on the Lewis acid sites and Brönsted acid sites, respectively [25]. The band at 1490 cm^{-1} is assigned to pyridine adsorbed on both Brönsted and Lewis acid sites. Therefore, the amounts of Lewis and Brönsted acid sites can be measured according to the absorption intensities of the bands at 1454 and 1545 cm^{-1}, respectively. As listed in Table 1, the ratio of strong Brönsted to Lewis acid sites was calculated based on Figure 2b [26]. Clearly, strong Brönsted acid sites far outnumber the Lewis acid sites for Mix-HBEA.

3.2 Catalytic Performance and Coke Formation of Catalyst

In order to investigate the conversion of 1-MN to 2-MN, the isomerization of 1-MN was performed over the Mix-HBEA catalyst at 573 K and 623 K. As demonstrated by past studies [8,27], the 1-MN conversion and 2-MN selectivity are decreased distinctly at temperature lower than 573 K and higher than 623 K, respectively. The other reaction conditions were as follows: WHSV was 1.3 h^{-1}, the time on stream (TOS) was 1 h and the carrier gas flow-rate was 20 mL/min. Table 2 lists the conversion results over the Mix-HBEA catalyst. Like in our previous study [11], disproportionation of 1-MN to NA and DMN is observed in conjunction with the isomerization of 1-MN to 2-MN.

At 573 K, the selectivity and yield of 2-MN over Mix-HBEA are 96.73 % and 67.10 %, respectively. These results suggest restrained disproportionation, as the 2-MN yield almost reaches the thermodynamic equilibrium of MN isomers. The results of NH_3-TPD and Py-FTIR indicate that both the weak and strong Lewis acid sites for Mix-HBEA are fewer in number than the strong Brönsted acid sites. These results imply that the Lewis and strong Brönsted acid sites in the catalyst act as active sites in the disproportionation [28,29] and isomerization [24,30] of 1-MN, respectively. When the reaction temperature increases from 573 to 623 K, the conversion of 1-MN is increased to 71.98 %, while the yield of disproportionation products is slightly enhanced [8]. As a result, the 2-MN selectivity decreases to 91.46 %, while the yield of 2-MN remains at a high level.

The stability of the Mix-HBEA catalyst with TOS was also tested at 573 K and 623 K. As shown in Figure 3a, the 1-MN conversion over Mix-HBEA decreases from 69.37 to 59.44 % af-

Table 1. Acidic properties of Mix-HBEA catalyst

Sample	Amount of acid[a], mmol/g			Strong B/L[b]
	Total acid	Weak acid	Strong acid	
Mix-HBEA	0.97	0.36	0.61	3.56

[a] Calculated based on Figure 2a. Weak acid: The amount of weakly acid sites calculated by integrating the desorption peak in the range 150-300 °C. Strong acid: The amount of strongly acidic sites calculated by integrating the desorption peak in the range 300-700 °C. Total acid: The sum of weak and strong acid.
[b] B/L: The ratio of strong Brönsted (B) to Lewis (L) acid site amounts calculated according to Figure 2b.

Table 2. Reaction results of 1-MN isomerization over Mix-HBEA catalyst

Reaction temperature, K	1-MN conversion, wt%	Product distribution[a], wt%				2-MN yield, wt%	Disproportionation yield, wt%	k_d[b], h^{-1}
		NA	2-MN	DMN	Others			
573	69.37	1.02	96.73	1.45	0.80	67.10	1.72	0.017
625	71.98	3.10	91.46	4.12	1.32	65.84	5.19	0.003

Reaction conditions: WHSV: 1.3 h^{-1}, time on stream: 1 h, carrier gas flow-rate: 20 mL/min
[a] Main products of 1-MN conversion: naphthalene (NA), 2-methylnaphthalene (2-MN), dimethylnaphthalene (DMN), and derivatives of polynuclear aromatic hydrocarbons (others).
[b] Deactivation rate calculated from Eq. (2).

ter 10 h TOS at 573 K, while that is still higher than 64.56 % after 30 h at 623 K. Then, the deactivation rate of catalyst is estimated for the quantification of isomerization stability. Assuming the adsorption equilibrium constant of two MN isomers are similar, the activity decay with TOS was expressed as follows:

$$\ln y_t - \ln y_0 = -k_d t \quad (2)$$

where, k_d is the deactivation rate, t is the TOS, and y_0 and y_t represent the conversion on the fresh and fouled catalyst, respectively [27]. The change in ln y_t with TOS is plotted in Figure 3b, and the values of k_d were calculated from the linear fittings. As listed in Table 2, the deactivation rate of Mix-HBEA at 623 K is less than one fifth that at 573 K, indicating that the deactivation rate decreases with increasing reaction temperature [31]. Thus, the isomerization stability of Mix-HBEA is improved significantly when the reaction temperature increases from 573 to 623 K. Considering the 1-MN conversion, 2-MN yield and isomerization stability, 623 K appears to be an appropriate reaction temperature for 1-MN isomerization over Mix-HBEA. The slightly low reaction selectively is not an obstacle, as the byproducts are eliminated in the crystallization process that follows.

The formation of coke deposits on the used catalysts was determined by TG under temperature programmed oxidation, and the results are shown in Figure 4. In the 40-200 °C range, the weight loss is associated with adsorbed moisture and gas in the catalysts. Above 200 °C, the steady weight of the fresh catalyst indicates none of carbonaceous deposits in unused Mix-HBEA. Nevertheless, in the 200-700 °C range, the weight of the used Mix-HBEA de-

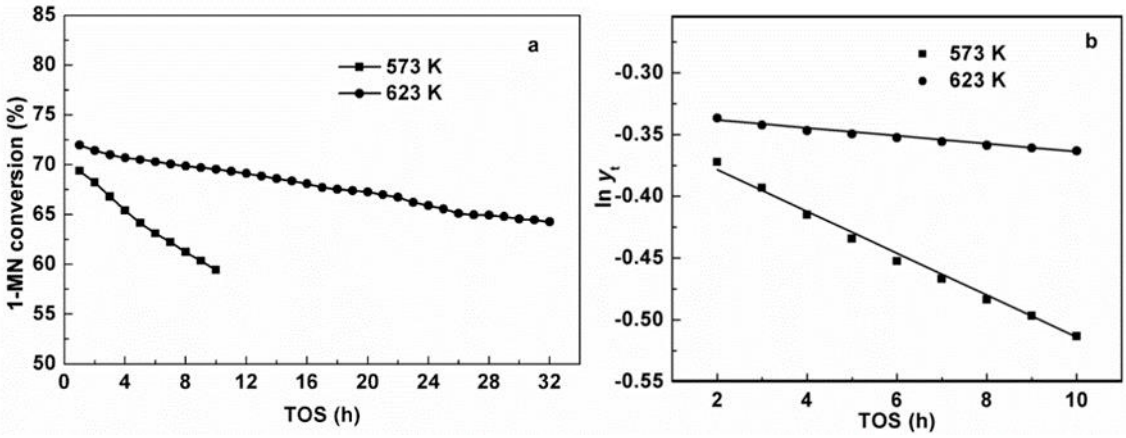

Figure 3. (a) Effects of TOS on 1-MN conversion over Mix-HBEA catalyst at 573 and 623 K; (b) Fitting of experimental points at 573 K and 623 K (reaction conditions: catalyst amount: 1.6 g, reaction pressure: 100 Kpa, WHSV: 1.3 h^{-1}, carrier gas flow-rate: 20 mL/min)

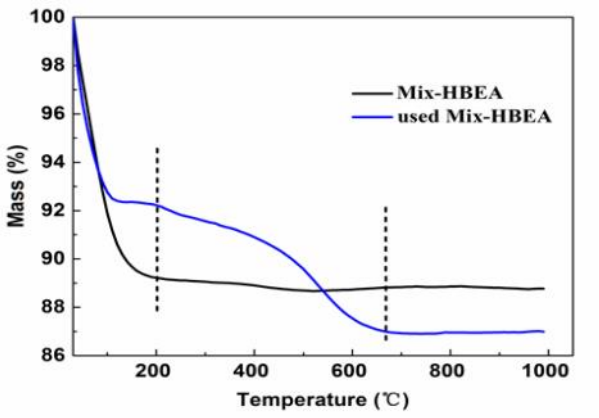

Figure 4. TG profile of fresh Mix-HBEA and used Mix-HBEA catalysts after 10 h TOS at 573 K (heating rate: 10 °C/min, atmosphere gas: O_2, 200 mL/min)

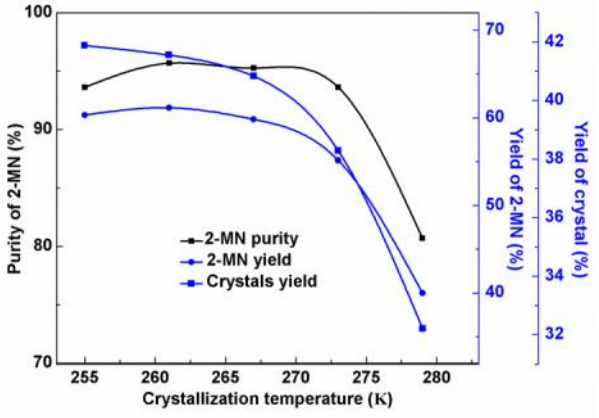

Figure 5. Effects of crystallization temperature on 2-MN purity, 2-MN yield and crystal yield (crystallization time: 180 min, filtration time: 20 min)

creases due to the oxidation of carbonaceous deposition in catalyst [26]. These coke deposited on the used catalyst account for the decrease of 1-MN conversion over Mix-HBEA after 10 h TOS at 573 K.

3.3 Crystallization

After the catalytic isomerization of 1-MN over the Mix-HBEA catalyst at 623 K, crystallization was carried out to refine 2-MN from the reaction product (see Table 2). As the quality of crystal products is remarkably influenced by different cooling conditions [32], the main factors including crystallization temperature, crystallization time and filtration time were examined in the crystallization process.

The effects of crystallization temperature on the separation process are plotted in Figure 5, where crystallization and filtration times were 180 and 20 min, respectively. The crystal yield decreases as the crystallization temperature increases. Meanwhile, as the crystallization temperature increases from 255 to 261 K, the 2-MN purity increases from 93.61 to 95.68 %, and the 2-MN yield also increases slightly. However, both the purity and yield of 2-MN decrease as the crystallization temperature increases further. These results suggest that crystallization at lower temperatures favors the nucleation and growth of 2-MN crystals, whereas the impurity would be incorporated into the growing crystals due to the burst nucleation at excessively low temperature [32,33]. Accordingly, a crystallization temperature of 261 K is optimal.

Figure 6 illustrates the effects of crystallization time on 2-MN purity and the yields of 2-MN and crystal, where the crystallization temperature was 261 K and the filtration time was 20 min. As crystallization time increases from 2 to 5 h, the 2-MN purity and the yields of 2-MN and crystal increase distinctly. However, the purity and yield of 2-MN decrease simultaneously as the crystallization time increases further, despite a slight increase in crystal yield. It is indicated that the impurity can grow into the crystal lattice easily because of the similarity of their structure with 2-MN molecule [34]. Therefore, 5 h represents an appropriate crystallization time in the crystallization process.

Figure 7 illustrates the effects of filtration time on 2-MN purity and yields of 2-MN and crystal, where the crystallization temperature was 261 K and the crystallization time was 5 h. The crystal yield decreases as the filtration time increases. Furthermore, as the filtration time increases from 5 to 20 min, 2-MN purity increases from 89.69 to 96.84 %, and 2-MN yield increases from 58.44 to 62.23 %. When the filtration time increases further from 20 to 30 min, both 2-MN purity and yield decrease. One possible reason for this phenomenon is that several crystals might be dissolved and filtrated in the impurity [35]. Thus, an advisable filtration time is 20 min.

The above results indicate that optimal parameters for the crystallization process are as follows: a crystallization temperature of 261 K, a crystallization time of 5 h, and a filtration time of 20 min. Under these conditions, the 2-MN purity and yield are 96.84 % and 62.23 %, respectively, and the crystal yield is 41.77 %. Moreover, the attaining filtrate of the crystallization process was crystallized again under the same conditions, after which the 2-MN pu-

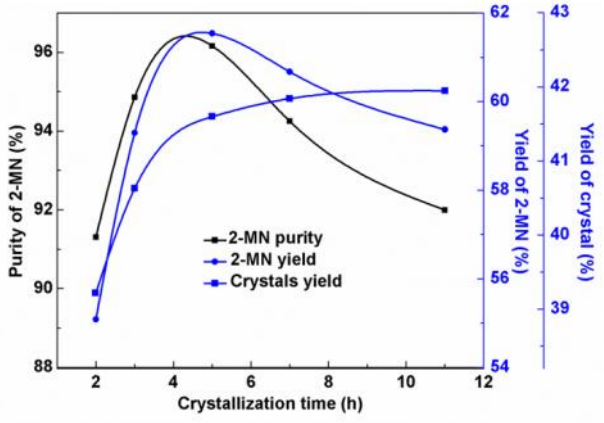

Figure 6. Effects of crystallization time on 2-MN purity, 2-MN yield and crystal yield (crystallization temperature: 261 K, filtration time: 20 min)

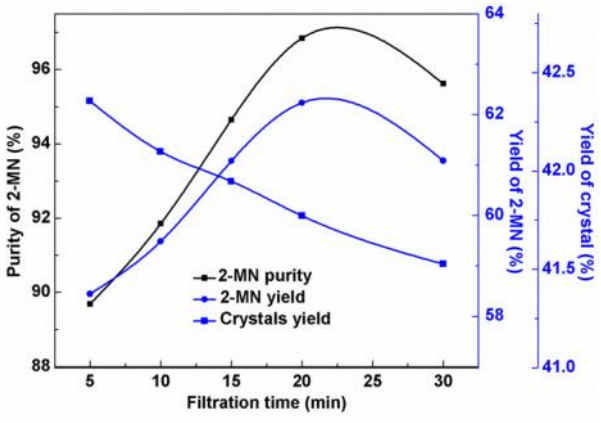

Figure 7. Effects of filtration time on 2-MN purity, 2-MN yield and crystal yield (crystallization temperature: 261 K, crystallization time: 5 h)

rity and yield are 96.25 % and 25.25 %, respectively, and the crystal yield is 17.05 %. Overall, after two consecutive crystallization processes, the 2-MN purity is 96.67 % and the total 2-MN yield of crystallization is 87.48 %. Thus, it is feasible to apply isomerization and crystallization to prepare highly purified 2-MN from 1-MN.

4. Conclusion

In this process, the isomerization of 1-MN over the Mix-HBEA catalyst and two-fold crystallizations to refine 2-MN were investigated. The Mix-HBEA catalyst presented fewer weak acid sites and strong Lewis acid sites than strong Brönsted acid sites, and it preserved the HBEA zeolite structure. At 623 K, the 2-MN yield was 65.84 % and the deactivation rate was 0.003 h^{-1} during the 1-MN isomerization process. After obtaining these results, the parameters for crystallization temperature, crystallization time and filtration time during the separation procedure were studied. Under optimal conditions, 2-MN attained 96.67 % purity, and the 2-MN yield reached 87.48 % after two consecutive crystallizations. Overall, the contribution of this paper lies in outlining a process by which residual 1-MN from C_{10} aromatics can be transformed to the more valuable 2-MN.

Acknowledgments

The project was supported by National Natural Science Foundation of China (31770629) and National Nonprofit Institute Research Grant of CAFINT (CAFYBB2017SY031).

References

[1] Pu, S.B., Inui, T. (1996). Synthesis of 2,6-Dimethylnaphthalene by Methylation of Methylnaphthalene on Various Medium and Large-pore Zeolite Catalysts. *Appl. Catal. A*, 146: 305-306.

[2] Lillwitz, L.D. (2001). Production of Dimethyl-2,6-naphthalenedicarboxylate: Precursor to Polyethylene Naphthalene. *Appl. Catal. A*, 221: 337-358.

[3] Arkhireyeva, A., Hashemi, S. (2001). Fracture Behaviour of Polyethylene Naphthalene (PEN). *Polymer*, 43: 289-300.

[4] Sun, H., Jiang, L., Gu, Z.G. (2015). Extract Methylnaphthalene from C10 Aromatics with Sidetrack Distillation and Continuous Crystallisation. *Mater. Res. Innovations*, 19: 573-578.

[5] Popova, Z., Yankov, M., Dimitrov, L., Chervenkov, I. (1994). Isomerization and Disproportionation of 1-Methylnaphthalene on Zeolites. *React. Kinet. Catal. Lett.*, 52: 51-58.

[6] Fedorynska, E., Winiarek, P. (1995). Isomerization of Alkylaromatic Hydrocarbons on Nickel-Boron-Alumina Catalysts. *React. Kinet. Catal. Lett.*, 54: 73-79.

[7] Takagi, Y., Nobusawa, T., Suzuki, T. (1995). Prevention and Estimation of Catalytic Deactivation in Isomerization of 1-Methylnaphthalene. *Kagaku Kogaku Ronbunshu*, 21: 1096-1103.

[8] Li, T.L., Liu, X.Y., Wang, X.S. (1997). Shape Selectivity for Disproportionation of Methylnaphthalene over Zeolite Hß. *Chin. J. Catal.*, 18: 221-224.

[9] Komatsu, T., Kim, J.H., Yashima, T. (1999). MFI-type Metallosilicates as Useful Tools to Clarify What Determines the Shape Selectivity of ZSM-5 Zeolites. *ACS Symp. Ser.*, 738: 162-180.

[10] Weitkamp, J., Neuber, M. (1991). Shape Selective Reactions of Alkylnaphthalenes in Zeolite Catalysts. *Stud. Surf. Sci. Catal.*, 60: 291-301.

[11] Sun, H., Shi, S.J., Gu, Z.G. (2017). Isomerization of Alkyl Naphthalene and Refining of 2-Methylnaphthalene. *Chin. J. Chem. Eng.*, 25: 149-152.

[12] Teng, H., Wang, J., Ren, X.Q., Chen, D.M. (2011). Disproportionation of Toluene by Modified ZSM-5 Zeolite Catalysts with High Shape-selectivity Prepared using Chemical Liquid Deposition with Tetraethyl Orthosilicate. *Chin. J. Chem. Eng.*, 19: 292-298.

[13] Zhang, C., Guo, X.W., Song, C.S., Zhao, S.Q., Wang, X.S. (2010). Effects of Steam and TEOS Modification on HZSM-5 Zeolite for 2,6-Dimethylnaphthalene Synthesis by Methylation of 2-Methylnaphthalene with Methanol. *Catal. Today*, 149: 196-201.

[14] Bai, G.Y., Han, J., Zhang, H.H., Liu, C., Lan, X.W., Tian, F., Zhao, Z., Jin, H. (2014). Friedel–Crafts Acylation of Anisole with Octanoic Acid over Acid Modified Zeolites. *RSC Adv.*, 4: 27116-27121.

[15] Chen, Z.H., Feng, Y.F., Tong, T.X., Zeng, A.W. (2014). Effects of Acid-modified HBEA Zeolites on Thiophene Acylation and the Origin of Deactivation of Zeolites. *Appl. Catal. A*, 482: 92-98.

[16] Bai, G.Y., Zhang, H.H., Li, T.Y., Dong, H.X., Han, J. (2014). Friedel–Crafts Acylation of Anisole with Hexanoic Acid Catalyzed by Hß Zeolite-supported Tungstophosphoric Acid. *Res. Chem. Intermed.*, 41: 5041-5048.

[17] Srivastava, R., Iwasa, N., Fujita, S., Arai, M. (2009). Dealumination of Zeolite Beta Catalyst under Controlled Conditions for Enhancing Its Activity in Acylation and Esterification. *Catal. Lett.*, 130: 655-663.

[18] Matsukata, M., Ogura, M., Osaki, T., Rao, P.R.H.P., Nomura, M., Kikuchi, E. (1999). Conversion of Dry Gel to Microporous Crystals in Gas Phase. *Top. Catal.*, 9: 77-92.

[19] Tamura, M., Shimizu, K.I., Satsuma, A. (2012). Comprehensive IR Study on Acid/Base Properties of Metal Oxides. *Appl. Catal. A*, 433-434: 135-145.

[20] Gu, Z.G., Jiang, L. (2013). A Integrated Separation Apparatus Including Homothermal Crystallization and Filtration. *CN 202682829 U* (in Chinese).

[21] Saxena, S.K., Viswanadham, N., Sharma, T. (2014). Breakthrough Mesopore Creation in BEA and Its Enhanced Catalytic Performance in Solvent-free Liquid Phase Tert-butylation of Phenol. *J. Mater. Chem. A.*, 2: 2487-2490.

[22] Esquivel, D., Cruz-Cabeza, A.J., Jiménez-Sanchidrián, C., Romero-Salguero, F.J. (2011). Enhanced Concentration of Medium Strength Brönsted Acid Sites in Aluminium-modified ß Zeolite. *Catal. Lett.*, 142: 112-117.

[23] Jin, D.F., Zhu, B., Hou, Z.Y., Fei, J.H., Lou, H., Zheng, X.M. (2007). Dimethyl Ether Synthesis via Methanol and Syngas over Rare Earth Metals Modified Zeolite Y and Dual Cu–Mn–Zn Catalysts. *Fuel*, 86: 2707-2713.

[24] Wang, Y.L., Xu, L., Yu, Z.X., Zhang, X.Z., Liu, Z.M. (2008). Selective Alkylation of Naphthalene with Tert-Butyl Alcohol over HY Zeolites Modified with Acid and Alkali. *Catal. Commun.*, 9: 1982-1986.

[25] Marques, J.P., Gener, I., Ayrault, P., Bordado, J.C., Lopes, J.M., Ribeiro, F.R., Guisnet, M. (2003). Infrared Spectroscopic Study of the Acid Properties of Dealuminated BEA Zeolites. *Microp. Mesop. Mater.*, 60: 251-262.

[26] Decolatti, H.P., Costa, B.O.D., Querini, C.A. (2015). Dehydration of Glycerol to Acrolein using H-ZSM5 Zeolite Modified by Alkali Treatment with NaOH. *Microp. Mesop. Mater.*, 204: 180-189.

[27] Rombi, E., Monaci, R., Solinas, V. (1999). Kinetics of Catalyst Deactivation. An Example: Methylnaphthalene Transformation. *Catal. Today*, 52: 321-330.

[28] Cañizares, P., Carrero, A. (2003). Dealumination of Ferrierite by Ammonium Hexafluorosilicate Treatment: Characterization and Testing in the Skeletal Isomerization of n-Butene. *Appl. Catal. A*, 248: 227-237.

[29] Wang, Y., Otomo, R., Tatsumi, T., Yokoi, T. (2016). Dealumination of Organic Structure-Directing Agent (OSDA) Free Beta Zeolite for Enhancing Its Catalytic Performance in n-Hexane Cracking. *Microp. Mesop. Mater.*, 220: 275-281.

[30] Kumsapaya, C., Bobuatong, K., Khongpracha, P., Tantirungrotechai, Y., Limtrakul, J. (2009). Mechanistic Investigation on 1,5- to 2,6-Dimethylnaphthalene Isomerization Catalyzed by Acidic ß Zeolite: ONIOM Study with an M06-L Functional. *J. Phys. Chem. C*, 113: 16128-16137.

[31] Guisnet, M., Costa, L., Ribeiro, F.R. (2009). Prevention of Zeolite Deactivation by Coking. *J. Mol. Catal. A: Chem.*, 305: 69-83.

[32] Ye, C.P., Ding, X.X., Li, W.Y., Mu, H., Wang, W., Feng, J. (2018). Determination of Crystalline Thermodynamics and Behavior of Anthracene in Different Solvents. *AIChE J.*, 64: 2160-2167.

[33] Ye, C.P., Zheng, H., Wu, T.T., Fan, M.M., Feng, J., Li, W.Y. (2014). Optimization of Solvent Crystallization Process in Obtaining High Purity Anthracene and Carbazole from Crude Anthracene. *AIChE J.*, 60: 275-281.

[34] Liu, J., Chang, Z.D., Sun, X.H., Shen, S.F., Lei, C., Liu, H.Z. (2006). Impurity Effects on the Crystallization of Avermectin B1a. *J. Cryst. Growth*, 291: 448-454.

[35] Cisternas, L.A., Vásquez, C.M., Swaney, R.E. (2006). On the Design of Crystallization-based Separation Processes: Review and Extension. *AIChE J.*, 52: 1754-1769.